Downloaded 09/15/17 to 217.144.243.100. Redistribution subject to SEG license or copyright; see Terms of Use at http://library.seg.org/

Large-scale 3D inversion of Towed Streamer EM data using the Gauss-Newton method

Jenny-Ann Malmberg, PGS, Johan Mattsson, PGS*

Summary

We present a newly developed 3D inversion code for Towed streamer EM data utilizing the Gauss-Newton method. The code is designed and implemented on a standard cluster of nodes to handle large-scale inversions of the order 25 million unknowns. The corresponding Jacobian matrix of about 2 Tb is split over the subscribed computational nodes in order to reduce the memory consumption on each node as well as to reduce the computational time. This enables the use of the full Gauss-Newton method on this amount of data.

The forward modeling part is based on a parallelized integral equation formulation of the electric field. The forward and inversion grids cover the entire survey area including bathymetry and down to 5 km below the sea surface.

The performance is demonstrated with an unconstrained anisotropic 3D inversion on Towed Steamer EM data over a survey area covering a total of 5206 sq. km, acquired in the Barents Sea in 2014. The survey consisted of 38 parallel acquisition lines with a spacing of 1.25 km and an average length of 115 km. The selected number of data observations for this case was 505820 with a total of 6 frequencies in the range from 0.2 to 2.2 Hz, 7226 shot points and 16 receiver offsets. The inversion grid consisted of 13 million cells and extended from the water column down to 5 km below the sea surface. The inversion ran 14 Gauss-Newton iterations and converged to a misfit of 3.7% with a geologically feasible anisotropic resistivity model.

Introduction

During the last couple of years, the size of CSEM acquisition areas has increased tremendously. The recently developed towed streamer EM system (McKay et. al., 2015), has proven to be efficient for regional size surveys in the order of 5000 km^2. As such survey sizes are becoming the CSEM survey standard in the industry, there is an increasing demand for fast and efficient 3D inversion codes that can process such large regions with reasonable amount of compute resource.

3D inversion of CSEM data over a large area implies that the inversion domain is discretized into millions of cells of unknown vertical and horizontal resistivity values. The number of data observations that are used in the inversion are hundreds of thousands. These amounts of unknowns and data observations are challenges in terms of computer RAM and computational time.

An example of large-scale inversion of CSEM data is given in (Zhdanov et. al., 2015). The paper describes the implementation of a 3D inversion algorithm using a Regularized Conjugate Gradient method for Towed Streamer EM data. It is demonstrated that feasible inversion results can be obtained for regional scale sub-surface domains within a few days computational time. A comparison between a similar conjugate gradient method and a Gauss-Newton method for large-scale node based CSEM inversion is presented in (Nguyen et. al., 2016). The conclusion is that the Gauss-Newton method captures the exponential attenuation of the electric field in a balanced way due to the explicit existence of the integrated sensitivity in the Gauss-Newton model update equation. This also implies faster convergence (fewer iterations) and a physically more correct result. The inversion is also less dependent on the start model. A successful Gauss-Newton implementation with Occam's regularization scheme for 2.5D inversion is presented in (Key et. al., 2014).

In this abstract, we present a newly developed 3D inversion code utilizing the Gauss-Newton method for Towed streamer EM data. The code is designed and implemented on a standard cluster of nodes to handle large-scale inversions of the order 10 million unknowns. The corresponding Jacobian matrix of 1-2 Tb is split over the subscribed nodes such that memory consumption on each node is reduced, and with it, the overall computational time. In addition, the non-zero entries in the Jacobian matrix are also reduced as a result of the limited sensitivity around each source position in a survey. This makes it possible to invert Towed Streamer EM data in 3D over regional scale areas using the Gauss-Newton method.

Theory and implementation

The inversion problem is formulated as a minimization problem with the following objective functional:

$$P(\mathbf{m}) = \left\| \mathbf{W}_d \left(\mathbf{E}(\mathbf{m}) - \mathbf{d} \right) \right\|_{L_2}^2 + \alpha R(\mathbf{m}) \qquad (1)$$

where

© 2017 SEG

Downloaded 09/15/17 to 217.144.243.100. Redistribution subject to SEG license or copyright; see Terms of Use at http://library.seg.org/

$\mathbf{m} = [\log(\sigma_1),\ldots,\log(\sigma_N)]$ = logarithm of the grid cell conductivities

$\mathbf{E}(\mathbf{m})$ = modelled electric field

$\mathbf{d}$ = measured electric field

$R(\mathbf{m})$ = regularization functional

α = regularization parameter

$\mathbf{W}_d$ = data weight matrix

The objective functional in (1) is minimized by using an iterative Gauss-Newton algorithm. The resulting linear system of equations for the update of the unknown conductivity vector $\mathbf{m}_k$ in iteration *k+1* is derived to:

$$\left(\alpha_k \mathbf{A} + \mathbf{S}_k^T \mathbf{S}_k\right)\Delta\mathbf{m}_k = \mathbf{S}_k^T \mathbf{W}_d\left(\mathbf{d} - \mathbf{E}_k\right) - \alpha_k \mathbf{A}\,\mathbf{m}_k \qquad (2)$$

where

$\mathbf{m}_{k+1} = \mathbf{m}_k + \Delta\mathbf{m}_k$

$\mathbf{A}$ = the corresponding regularization matrix

$\mathbf{S}(\mathbf{m}_k) = \mathbf{W}_d\mathbf{J}(\mathbf{m}_k)$

$\mathbf{J}(\mathbf{m}_k)$ = Jacobian matrix

The forward modeling part is based on an integral equation formulation in the frequency domain according to:

$$\mathbf{E}(\mathbf{r}) = \mathbf{E}^b(\mathbf{r}) + \int_V \mathbf{G}_e(\mathbf{r},\mathbf{r}')\cdot\left(\left(\sigma(\mathbf{r}') - \sigma^b(\mathbf{r}')\right)\cdot\mathbf{E}(\mathbf{r}')\right)dV(\mathbf{r}') \qquad (3)$$

where

$\mathbf{G}_e(\mathbf{r},\mathbf{r}',\omega)$ = The electric Green's tensor of the 1D background model.

$\sigma(\mathbf{r}')$ = The conductivity tensor of the 3D model.

$\sigma^b(\mathbf{r}')$ = The conductivity tensor of the 1D background model

The conductivity tensors are currently restricted to transverse isotropic anisotropy. The forward grid as well as the inversion grid are the same and cover the entire survey area including bathymetry. Figure 1 shows a vertical cross section of an inversion grid as well as a typical source and receiver configuration in the seawater for the Towed Streamer EM system. The depth extension of the grid below the seafloor is normally 4-5 km.

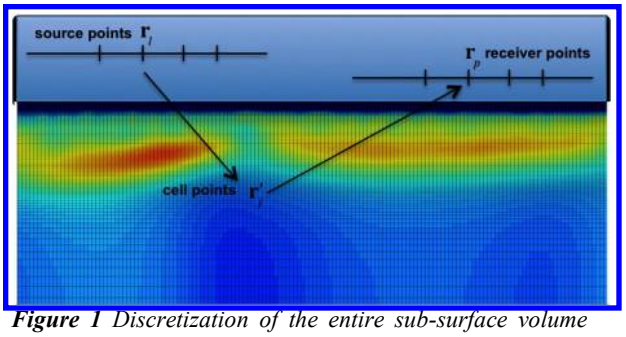

Figure 1 *Discretization of the entire sub-surface volume underneath the survey lines. The inversion grid cells are about 10 m thick at the seafloor then gradually thicker deeper down.*

The regularization functional $R(\mathbf{m})$ in the objective function (1) can be formulated in a number of ways. See (Zhdanov et. al., 2014) for examples of the regularization functional. The smoothing regularization expressed as the gradient of the model across the inversion cells as given in (Key et. al., 2014) is also used in the implementation described here. In fact, the regularization functional in this code is:

$$R(\mathbf{m}) = w_0\left\|\mathbf{m} - \mathbf{m}_{apriori}\right\|_{L_2}^2 + w_x\left\|\partial_x\mathbf{m}\right\|_{L_2}^2 + w_y\left\|\partial_y\mathbf{m}\right\|_{L_2}^2 + w_z\left\|\partial_z\mathbf{m}\right\|_{L_2}^2 \qquad (4)$$

where w_0, w_x, w_y and w_z are weight parameters.

The first term in (4) is regularization towards an a priori model whereas the other terms are smoothing of the model in the x, y and z-directions. The smoothing is accomplished by minimizing the model variation between adjacent inversion cells.

The regularization parameter α in the objective function (1) is determined by so-called geometric progression, also referred to as adaptive regularization in (Zhdanov et. al., 2014). This means that the parameter is decreased at each Gauss-Newton iteration according to:

$$\alpha = \alpha_1 q^{k-1} \qquad (5)$$

k = iteration index and q = step length

The step length q and the initial regularization parameter α_1 are given as input at the start of the inversion.

© 2017 SEG

Downloaded 09/15/17 to 217.144.243.100. Redistribution subject to SEG license or copyright; see Terms of Use at http://library.seg.org/

The horizontal and vertical conductivity components of the Jacobian matrix in (2) are calculated according to:

$$J_{k,(ipl)j,h} = E^{x}_{k,(ijl)} E^{x}_{k,(ijp)} + E^{y}_{k,(ijl)} E^{y}_{k,(ijp)}$$
$$J_{k,(ipl)j,v} = E^{z}_{k,(ijl)} E^{z}_{k,(ijp)} \quad (6)$$

where

k = iteration index , j = cell point index
(ipl) = data indicies where i = frequency index
p = receiver index and l = source point index
h = horizontal conductivity or
v = vertical conductivity

The expressions in (6) can be derived from the corresponding continuous case, i.e. without a discrete inversion grid, as shown in (Abubakar et. al., 2008). Basically the Jacobian elements are composed of the products of the electric fields at all cell mid-points with the source in the source points and at the receiver points, respectively, as can be seen from the index notation in (6).

The number of forward modelling calculations for a large scale CSEM inversion is huge and can be reduced by only calculating the electric field within a predetermined box of sensitivity around each source position. This results in a banded Jacobian matrix with heavily reduced number of non-zero elements. The computational time is also reduced in this way. Moreover, the electric field computations are also parallelised over both frequencies and source positions to reduce the computational time further. The matrix in the linear system of equations when solving the integral equation for the electric field is also shared in memory within each node for each frequency.

The linear system in (2) is solved with a standard conjugate gradient algorithm; the matrix in the system is split and distributed over the subscribed processes. If P processes are used, the matrix is divided into P sets of rows, which are distributed to the P processes. This means that M/P rows of the Jacobian matrix, (the total number of rows is M), are assembled and multiplied by the solution vector at each process in every iteration of the conjugate gradient algorithm when solving equation (2). This reduces the required RAM per node with a factor equal to the number of nodes. The parallelization of the matrix assembling as well as matrix vector multiplication over all processes also reduces the computational time significantly. A similar solution method for the Gauss-Newton update equation when the number of cells is large is explained in (Chevalier and Pellegrini, 2007).

Unconstrained 3D inversion of a large scale towed EM survey

To demonstrate the performance of the 3D inversion code, an unconstrained 3D inversion was run on Towed Steamer EM data over a survey area covering a total of 5206 sq. km, acquired in the Barents Sea in 2014. The survey area consisted of 38 survey lines with a line spacing of 1.25 km and an average length of 115 km. The number of data observations was 505820 with a total of 6 frequencies in the range 0.2 to 2.2 Hz, 7226 shot points and up to 16 sensors. The shot spacing was on average 500 m.

The inversion grid consisted of 13 million cells (217 x 604 x 111) that were 250 m x 250 m in horizontal direction and ranged between 7 m to 149 m in the vertical direction. The grid extended down to 5 km below the sea surface. The upper boundary of the inversion domain was located 1 m above the shallowest point of the bathymetry at 204 m. Cells located in the water were masked, allowing for inversion in the sediment only. In this way, the bathymetry was accurately modelled.

The inversion was started from a simple anisotropic half space. No a priori model was used. The following start model was used in the inversion, containing three layers in the water:

Upper water layer (sea surface – 63 m)	3.46 S/m
Middle water layer (63 m – 200 m)	3.18 S/m
Lower water layer (200 m – sea bed)	2.97 S/m
Sediment layer (horizontal)	0.18 S/m
Sediment layer (vertical)	0.04 S/m

The dimensions of the inversion problem resulted in a 1.5 Tb Jacobian matrix. The inversion was run on a compute cluster on 80 nodes and 10 processes per node, resulting in a distribution of the computational load over 800 processes as described above. Each cluster node had 10 dual cores with 2.8 GHz Intel Xeon processors and 128 GB memory. In order to utilize the full capacity of the cores, threading was also applied.

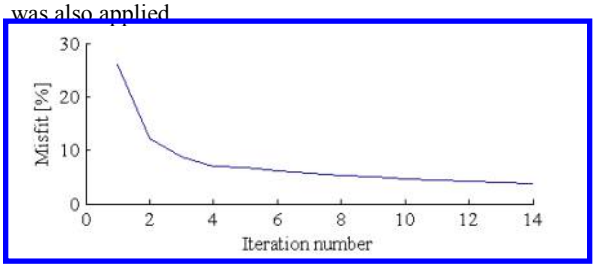

Figure 2 *The misfit corresponding to the 14 Gauss Newton iterations in the 3D inversion.*

© 2017 SEG

Downloaded 09/15/17 to 217.144.243.100. Redistribution subject to SEG license or copyright; see Terms of Use at http://library.seg.org/

As shown in figure 2, the misfit of the initial model was 26%. The inversion ran 14 Gauss Newton iterations and converged to a misfit of 3.7%, demonstrating the efficiency of the inversion methodology. The inversion ran for one week with an average iteration time of 11.5 hours, with the fastest iteration time at 6 hours and the longest at 17 hours. Scale tests indicate that it should be possible to reduce the runtime significantly, by adding more compute nodes.

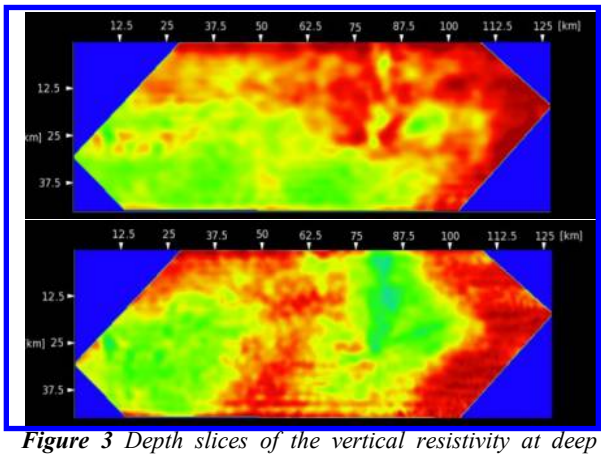

Figure 3 *Depth slices of the vertical resistivity at deep (top) and shallow (bottom) depth.*

In figure 3, an example of depth slices of the vertical resistivity volume at deep- (top) and shallow (bottom) depth is shown. High resistivity is coloured in red and lower in blue/green. A closer examination of the volume shows that the inversion methodology can successfully recover resistivity structures that correlate with observations from seismic acquisition in the same area.

Example cross sections in depth of the vertical (top), and horizontal (bottom) resistivities of the modelled volume are shown in figure 4. The sections have been overlain on corresponding seismic sections. The colour scales of the resistivity sections have been selected to show characteristic features of the horizontal and vertical resistivities and are therefore not the same. Some of these features include the recovery of expected depth trend in resistivity such as a general increase with depth in the horizontal resistivity, as well as both resistive and conductive features following the lateral depth trend e.g. the relatively low (horizontal) resistivity zone between 500 and 1000 m depth.

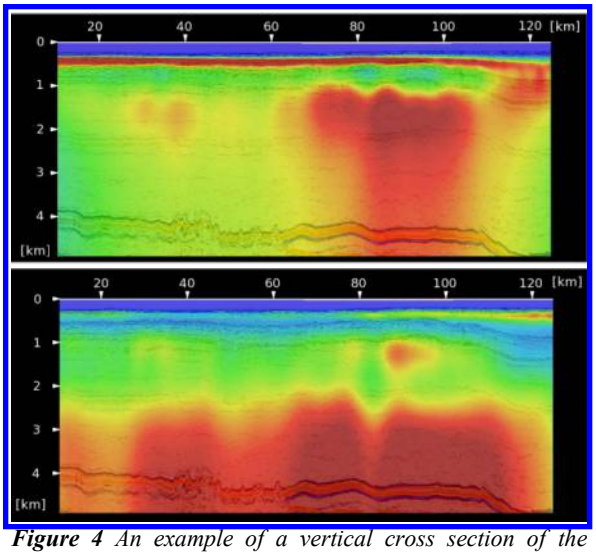

Figure 4 *An example of a vertical cross section of the vertical- (top) and horizontal (bottom) resistivities overlain with corresponding seismic sections. The colour scales have been selected to show characteristics of the anisotropic resistivity model, and are therefore not the same.*

Conclusions

We have shown how the Gauss Newton minimization method can be implemented in an efficient way to enable large-scale 3D inversion of Towed Streamer EM data. The real data example demonstrates that 3D inversion of survey areas in the order of 5000 km^2 can be run on a standard cluster of reasonable size within a week. The inversion generated a resistivity volume that was consistent with the known geology.

Acknowledgement

The authors would like to thank PGS for the permission to publish this work.

© 2017 SEG

EDITED REFERENCES

Note: This reference list is a copyedited version of the reference list submitted by the author. Reference lists for the 2017 SEG Technical Program Expanded Abstracts have been copyedited so that references provided with the online metadata for each paper will achieve a high degree of linking to cited sources that appear on the Web.

REFERENCES

Abubakar A., T. M Habashy, V. L Druskin, L. Knizhnerman, and D. Alumbaugh, 2008, 2.5D forward and inverse modeling for interpreting low-frequency electromagnetic measurements, Geophysics, **73**, no. 4, F165–F177, https://doi.org/10.1190/1.2937466.

Chevalier C., and F. Pellegrini, 2008, PT-SCOTCH: A tool for efficient parallel graph ordering: Parallel Computing, **34**, 318–331, https://doi.org/10.1016/j.parco.2007.12.001.

Key, K., Z. Du, J. Mattsson, A. McKay and J. Midgley, 2014, Anisotropic 2.5D inversion of Towed Streamer EM data from three North Sea fields using parallel adaptive finite elements: 76th Annual International Conference and Exhibition, EAGE, Extended Abstracts, https://doi.org/10.3997/2214-4609.20140730.

McKay, A., J. Mattsson, and Z. Du, 2015, Towed Streamer EM — Reliable recovery of sub-surface resistivity, First Break, **33**, 75–86.

Nguyen A. K., J. I. Nordskag, T. Wiik, A. K. Bjørke, L. Boman, O. M. Pedersen, J. Ribaudo, and R. Mittet, 2016, Comparing large-scale 3D Gauss-Newton and BFGS CSEM inversions: SEG.

Zhdanov, M., M. Endo, D. Sunwall, and J. Mattsson, 2015, Advanced 3D imaging of complex geo-electrical structures using towed streamer EM data over the Mariner field in the North Sea, First Break, **33**, 59–63.

Zhdanov, M. S., M. Endo, D. Yoon, J. Mattsson, and J. Midgley, 2014, Anisotropic 3D inversion of towed streamer EM data: Case study from the Troll West Oil Province: Interpretation, **2**, SH97–SH113, https://doi.org/10.1190/INT-2013-0156.1.

Downloaded 09/15/17 to 217.144.243.100. Redistribution subject to SEG license or copyright; see Terms of Use at http://library.seg.org/